cGMP Inhibits TGF-β Signaling by Sequestering Smad3 with Cytosolic β2-Tubulin in Pulmonary Artery Smooth Muscle Cells

Kaizheng Gong, Dongqi Xing, Peng Li, Robert H. Hilgers, Fadi G. Hage, Suzanne Oparil, and Yiu-Fai Chen

Vascular Biology and Hypertension Program (K.G., D.X., P.I., R.H.H., F.G.H., S.O., Y.-F.C.), Department of Medicine, University of Alabama at Birmingham, Birmingham, Alabama 35294; and Department of Cardiology (K.G.), The Second Clinical Medical School, Yangzhou University, Yangzhou 225001, China

Atrial natriuretic peptide (ANP) and TGF-β play counterregulatory roles in pulmonary vascular adaptation to chronic hypoxia. We have demonstrated that ANP-cyclic GMP (cGMP)-protein kinase G (PKG) signaling inhibits TGF-β signaling by blocking TGF-β-induced nuclear translocation of mothers against decapentaplegic homolog (Smad)3 in pulmonary artery smooth muscle cells (PASMC). The current study tested the novel hypothesis that activation of the ANP-cGMP-PKG pathway limits TGF-β-induced Smad3 nuclear translocation by enhancing Smad3 binding to cytosolic anchoring proteins in isolated pulmonary artery smooth muscle cells. Cells were pretreated with vehicle or cGMP and then exposed to TGF-β1 treatment. Cytosolic fractions were isolated and immunoprecipitated with a selective anti-Smad3 antibody. Differential proteomic analysis of the cytosolic Smad3-interacting proteins by two-dimensional differential in-gel electrophoresis and mass spectroscopy followed by coimmunoprecipitation and immunostaining demonstrated that Smad3 was bound to β2-tubulin in a TGF-β1/cGMP-dependent manner: binding of Smad3 to β2-tubulin was decreased by TGF-β1 and increased by cGMP treatment. A site-directed mutagenesis study demonstrated that mutating Smad3 at Thr388, but not Ser309, two potential sites of PKG-induced hyperphosphorylation, inhibited cGMP-induced Smad3 binding to β2-tubulin. Further, luciferase reporter analysis showed that muation of T388 in Smad3 abolished the inhibitory effect of cGMP on TGF-β1-induced plasminogen activator inhibitor-1 (PAI-1) transcription. In addition, disruption of β2-tubulin with the microtubule depolymerizers nocodazole and colchicine promoted Smad3 dissociation from β2-tubulin, increased both TGF-β1-induced Smad3 nuclear translocation and PAI-1 mRNA expression, and abolished the inhibitory effects of cGMP on these processes. In contrast, the microtubule stabilizers paclitaxel and epothilone B increased cytosolic Smad3 binding to β2-tubulin and enhanced the inhibitory effect of cGMP on Smad3 nuclear translocation and PAI-1 expression in response to TGF-β1. These provocative findings suggest that sequestering Smad3 by β2-tubulin in cytosol is a key mechanism by which ANP-cGMP-PKG signaling interferes with downstream signaling from TGF-β and thus protects against pulmonary arterial remodeling in response to hypoxia stress. **(*Molecular Endocrinology* 25: 1794–1803, 2011)**

Under chronic hypoxic stress, endogenous atrial natriuretic peptide (ANP) and TGF-β signaling are activated and play counterregulatory roles in pathological pulmonary arterial remodeling (1–3). We have previously shown that ANP-null mice develop more severe pulmonary hypertension and vascular remodeling than wild-type animals in response to chronic hypoxic exposure (1). In contrast, disruption of TGF-β signaling by inducible

ISSN Print 0888-8809 ISSN Online 1944-9917
Printed in U.S.A.

doi: 10.1210/me.2011-1009 Received March 18, 2011. Accepted July 22, 2011.
First Published Online August 25, 2011

Abbreviations: ANP, Atrial natriuretic peptide; cGMP, cyclic GMP; C.I., confidence interval; Co-IP, coimmunoprecipitation; DAPI, 4′,6-diamidino-2-phenylindole; 2D-DIGE, two-dimensional differential in-gel electrophoresis; GAPDH, glyceraldehyde-3-phosphate dehydrogenase; HDAC1, histone deacetylase 1; IB, immunoblotting; MS, mass spectroscopic; PAI, plasminogen activator inhibitor; PASMC, pulmonary artery smooth muscle cell; PKG, protein kinase G; Smad, mothers against decapentaplegic homolog; TOF, time-of-flight.

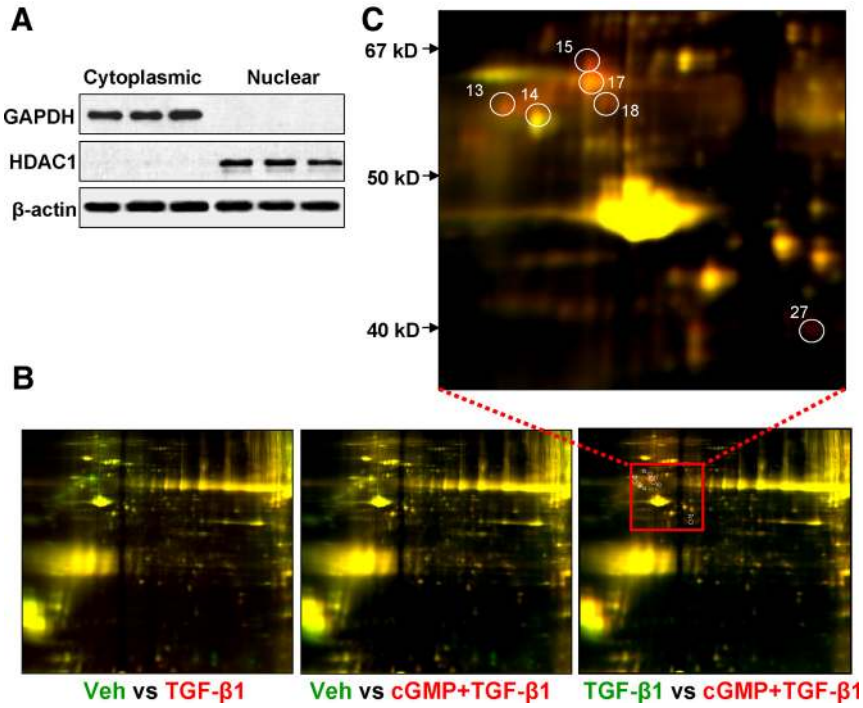

FIG. 1. Proteomic profiling of cytosolic Smad3-binding proteins in PASMC in absence or presence of cGMP and TGF-β1. Serum-starved PASMC were pretreated with cGMP (0.5 mM) or vehicle (Veh) for 1 h and then exposed to TGF-β1 (2 ng/ml) for 1 h. The cytoplasmic and nuclear fractions were isolated and purified. A, IB analysis for assessment of the quality of extracted proteins using GAPDH and HDAC1 as markers of the cytosolic and nuclear fractions, respectively. B, Images of differential expression of cytosolic Smad3-binding proteins in Veh, TGF-β1, and cGMP + TGF-β1 groups by 2D-DIGE analysis. *Green spots* represent down-regulated proteins, whereas *red spots* indicate up-regulated proteins. Proteins were separated according to molecular weight and isoelectric point. C, A locally magnified picture of the area of interest. *Circles and numbers* refer to spots in which proteins were identified by MS.

overexpression of a dominant negative mutant of TGF-β receptor type II effectively prevents hypoxia-induced pulmonary hypertension, right ventricular hypertrophy, pulmonary arterial remodeling and muscularization, and expression of extracellular matrix in mice (2). In subsequent studies, we provided direct evidence to support functional counterregulation between endogenous ANP-cyclic GMP (cGMP)-protein kinase G (PKG) and TGF-β-mothers against decapentaplegic homolog (Smad) signaling in the pulmonary vascular adaptation to chronic hypoxia. We observed that treatment with either ANP or cGMP inhibits TGF-β1-induced Smad nuclear translocation, a key molecular event in the TGF-β signaling pathway, and reduces TGF-β1-induced expression of extracellular matrix molecules in isolated rat pulmonary artery smooth muscle cells (PASMC) (3).

In the present study, we elucidated the molecular mechanism by which cGMP inhibits TGF-β-induced nuclear translocation of Smad3 in isolated PASMC. Specifically, we tested the novel hypothesis that activation of the cGMP-PKG pathway limits TGF-β-induced nuclear translocation of Smad3 by enhancing Smad3 binding to cytosolic anchoring proteins. Using two-dimensional differential in-gel electrophoresis (2D-DIGE) and mass spectroscopic (MS) analyses, confirmed by coimmunoprecipitation (Co-IP) and immunostaining analyses, we demonstrated that cytosolic sequestration of Smad3 with the cytoskeletal protein β2-tubulin is a key mechanism, by which cGMP-PKG signaling interferes with downstream signal transduction from TGF-β in PASMC.

Results

Two-dimensional differential proteomic and MS analyses of cytosolic Smad3-anchoring proteins in TGF-β1-treated PASMC with or without cGMP pretreatment

To test our novel hypothesis that cGMP treatment limits TGF-β-induced Smad3 nuclear translocation by enhancing Smad3 binding to cytosolic anchoring proteins, we carried out a differential proteomic analysis to identify candidate cytosolic proteins for Smad3 binding. Isolated PASMC were pretreated with cGMP or vehicle for 1 h followed by exposure to TGF-β1 or vehicle for 1 h, and the cytosolic and nuclear proteins were isolated. Using glyceraldehyde-3-phosphate dehydrogenase (GAPDH) and histone deacetylase 1 (HDAC1) as markers of the cytosolic and nuclear fractions (4), respectively, we demonstrated that the isolated cytosolic fraction was not contaminated with nuclear proteins (Fig. 1A). Cytosolic extracts were immunoprecipitated with anti-Smad3 to enrich for Smad3-interacting proteins, and the proteomes were profiled by 2D-DIGE. Differential proteomic expression among vehicle, TGF-β1, and cGMP + TGF-β1-treated cells was analyzed by DeCyder image analysis software.

TGF-β1 treatment significantly decreased Smad3 binding to 48 cytosolic proteins and increased Smad3 binding to four cytosolic proteins compared with vehicle-treated cells (Fig. 1B, *left image*, and Supplemental Table 1, published on The Endocrine Society's Journals Online web site at http://mend.endojournals.org). cGMP + TGF-β1 treatment increased Smad3 binding to 13 proteins and decreased Smad3 binding to 39 proteins compared with vehicle (Fig. 1B, *middle image*, and Supplemental Table 1). To test the

TABLE 1. MS analysis of proteins of interest on 2D-DIGE gel

Spot ID	Protein name	Accession no.	MW (Da)	PI	Peptide counts	Protein score	Protein score % C.I.	Fold increase (cGMP + TGF-β1 *vs.* TGF-β1)
14	Tubulin β-2 C chain	gi 40018568	49769	4.79	21	184	100	3.33
27	BRCC36	gi 198278575	32994.7	5.84	10	99	100	2.42
15	Vimentin, isoform-β	gi 149021114	53668.1	5.06	29	256	100	2.24
13	Vimentin, isoform-β	gi 149021114	53668.1	5.06	25	256	100	2.21
17	Vimentin, isoform-β	gi 149021114	53668.1	5.06	29	290	100	2.13
18	Aldose reductase	gil6978491	35774.3	6	6	41	43	2.0

MW, Molecular weight; PI, isoelectric point. β2-Tubulin is a cytoskeletal protein. BRCC36 and vimentin are both cytosolic and nuclear proteins (24, 25). The low protein score (43% C.I.) of aldose reductase suggests a possibility of incorrect protein identification. ID, Identification.

effect of cGMP pretreatment on Smad3 interaction with cytosolic proteins in the presence TGF-β1, we focused on the comparison between the cGMP + TGF-β1 group and the TGF-β1 group. cGMP + TGF-β1 treatment increased Smad3 binding to 44 proteins and decreased Smad3 binding to eight proteins compared with TGF-β1 alone (Fig. 1B, *right image*, and Supplemental Table 1).

Among the 44 proteins that showed increased Smad3 binding with cGMP pretreatment, we selected six with fold increased more than 2 for further MS analysis (Fig. 1C). MS analysis identified the six proteins of interest as the cytoskeletal protein β2-tubulin, a lys-63-specific deubiquitinase BRCC36, vimentin and its three isoforms, and aldose reductase (Table 1). Because it has been reported previously that Smad3 binds to cytosolic microtubules in endothelial and epithelial cells (5, 6) and because cGMP treatment resulted in the highest fold (3.33) increase in Smad3 binding to β2-tubulin in our study, we focused on the Smad3-β2-tubulin interaction for further investigation.

TGF-β1 treatment decreases, but cGMP treatment increases, Smad3 binding to β2-tubulin in PASMC

We used a reciprocal Co-IP assay to further examine the Smad3-β2-tubulin interaction in PASMC. Quiescent PASMC were pretreated with cGMP or vehicle for 1 h and exposed to TGF-β1 or vehicle for 1 h. Whole cell protein extracts were subjected to IP with anti-Smad3 antibody followed by immunoblotting (IB) with anti-β2-tubulin antibody (Fig. 2A). β2-Tubulin was bound to Smad3 in vehicle-treated cells. TGF-β1 treatment led to a significant decrease in β2-tubulin binding to Smad3. cGMP treatment caused a marked increase in β2-tubulin binding to Smad3 compared with vehicle treatment and abolished the inhibitory effect of TGF-β1 on β2-tubulin binding to Smad3. In the reverse Co-IP, whole cell protein extracts were subjected to IP with selective anti-β2-tubulin antibody, followed by IB with anti-Smad3 antibody (Fig. 2B). We confirmed that Smad3 constitutively binds to β2-tubulin in the vehicle-treated cells. TGF-β1 treatment significantly decreased the binding of Smad3 to β2-tubulin, whereas cGMP treatment significantly increased Smad3 binding to β2-tubulin compared with vehicle treatment. Importantly, cGMP pretreatment abolished the TGF-β1-induced dissociation of Smad3 from β2-tubulin. ANP treatment mimicked the enhancing effects of cGMP on the interaction between Smad3 and β2-tubulin and inhibited TGF-β1-induced plasminogen activator inhibitor (PAI)-1 mRNA expression (Supplemental Fig. 1). These results suggest that the ANP-cGMP-PKG pathway and TGF-β signaling play counterregulatory roles in regulating the constitutive binding of Smad3 to β2-tubulin in PASMC.

TGF-β1 treatment decreases, but cGMP treatment increases, the colocalization of cytosolic Smad3 with β2-tubulin in PASMC

To test whether Smad3 colocalizes with β2-tubulin in the cells, we performed immunofluorescence staining with anti-Smad3 and anti-β2-tubulin antibodies. In vehicle-treated cells, Smad3 was distributed uniformly in the cytosol and nucleus, whereas β2-tubulin formed a typical filament-like structure around the nucleus (Fig. 3). Merging the images clearly demonstrated colocalization of Smad3 and β2-tubulin. Consistent with the results of the Co-IP studies, TGF-β1 treatment caused a significant reduction in colocalization of Smad3 and β2-tubulin and led to a significant nuclear accumulation of Smad3. In contrast, cGMP treatment significantly increased Smad3 colocalization with β2-tubulin compared with the vehicle control group. Further, cGMP pretreatment significantly blocked TGF-β1-induced Smad3 nuclear accumulation and increased Smad3 colocalization with β2-tubulin in the cytosol compared with the TGF-β1-treated group.

cGMP-induced hyperphosphorylation of Smad3 enhances the interaction between Smad3 and β2-tubulin

Our previous results suggested that PKG activation-induced hyperphosphorylation of Smad3 at Ser309 and Thr388 residues may play a critical role in the prevention of Smad3 nuclear translocation (7). To test the hypothesis

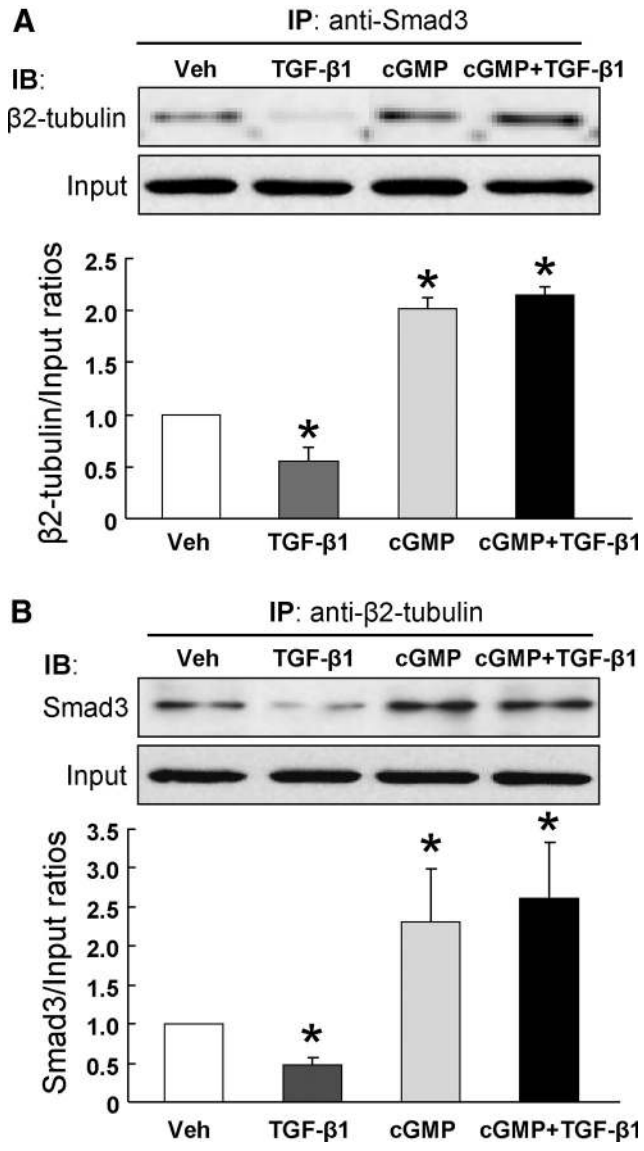

FIG. 2. TGF-β1 reduced, and cGMP enhanced, Smad3-β2-tubulin interaction in PASMC. Serum-starved PASMC were pretreated with cGMP (0.5 mM) or vehicle (Veh) for 1 h and then exposed to TGF-β1 (2 ng/ml) for 1 h. Whole cell extracts were subjected to reciprocal Co-IP analysis with anti-Smad3 (A) and anti-β2-tubulin (B) antibodies. Representative IB of the immunoprecititates from three independent experiments are shown in the *top of panels*. After IB analysis, the blot was stripped and then probed with anti-Smad3 or anti-β2-tubulin, respectively (input). Results are means ± SEM; *, $P < 0.05$ *vs.* vehicle.

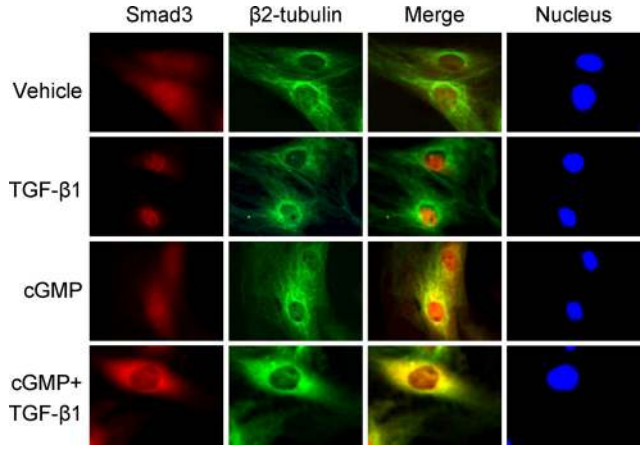

FIG. 3. Effects of TGF-β1 and cGMP on colocalization of Smad3 and β2-tubulin in PASMC. Serum-starved PASMC were pretreated with cGMP (0.5 mM) or vehicle for 1 h and then exposed to TGF-β1 (2 ng/ml) for 1 h. The cells were fixed and subjected to double immunostaining with anti-Smad3 (*red*) and anti-β2-tubulin (*green*) antibodies. Nuclei were stained with DAPI. After merging, colocalization is presented in *yellow*.

that hyperphosphorylated Smad3 binds to β2-tubulin in the presence of cGMP, wild-type Smad3, S309G-Smad3, T388A-Smad3, or the empty vector were transiently transfected into HEK293 cells. Overexpression of Smad3 was confirmed by Western blot analysis. Compared with cells transfected with the empty vector, overexpression of Smad3 increased Smad3 binding to β2-tubulin in vehicle-treated cells. cGMP treatment potentiated Smad3 binding to β2-tubulin in cells transfected with wild-type Smad3 or S309G-Smad3 and significantly inhibited TGF-β1-induced PAI-1 mRNA expression (Supplemental Fig. 2). In contrast, mutation of Smad3 at the Thr388 significantly attenuated cGMP-induced Smad3 binding to β2-tubulin (Fig. 4A). Luciferase assay demonstrated that mutation of Smad3 at the S309 residue did not alter cGMP-induced inhibition of transcriptional activity of PAI-1 in the presence of TGF-β1 in PASMC. In contrast, mutation of Smad3 at Thr388 residue abolished the inhibitory effect of cGMP (Fig. 4B). These results suggest that the Thr388 residue of Smad3 plays an essential role in mediating cGMP-induced enhancement of Smad3 binding to β2-tubulin and inhibition of PAI-1 transcriptional activity in response to TGF-β1 treatment.

Nocodazole pretreatment abolishes the inhibitory effect of cGMP on TGF-β1-induced PAI-1 mRNA expression

To test the functional significance of β2-tubulin binding in preventing nuclear translocation of Smad3, we used the microtubule depolymerizer nocodazole to disrupt the β2-tubulin (5). Incubation of vehicle-treated cells with nocodazole led to the formation of punctuate-like structures, in which cytosolic β2-tubulin was localized, in addition to increased Smad3 accumulation in the nucleus (Fig. 5A). TGF-β1 treatment further enhanced nocodazole-induced Smad3 nuclear translocation. Importantly, nocodazole pretreatment abolished cGMP-induced Smad3 binding to β2-tubulin. cGMP pretreatment had no effect on TGF-β1-induced Smad3 nuclear accumulation in nocodazole-treated cells. These results provide pivotal evidence that the structural integrity of β2-tubulin has an essential role in mediating its interaction with Smad3.

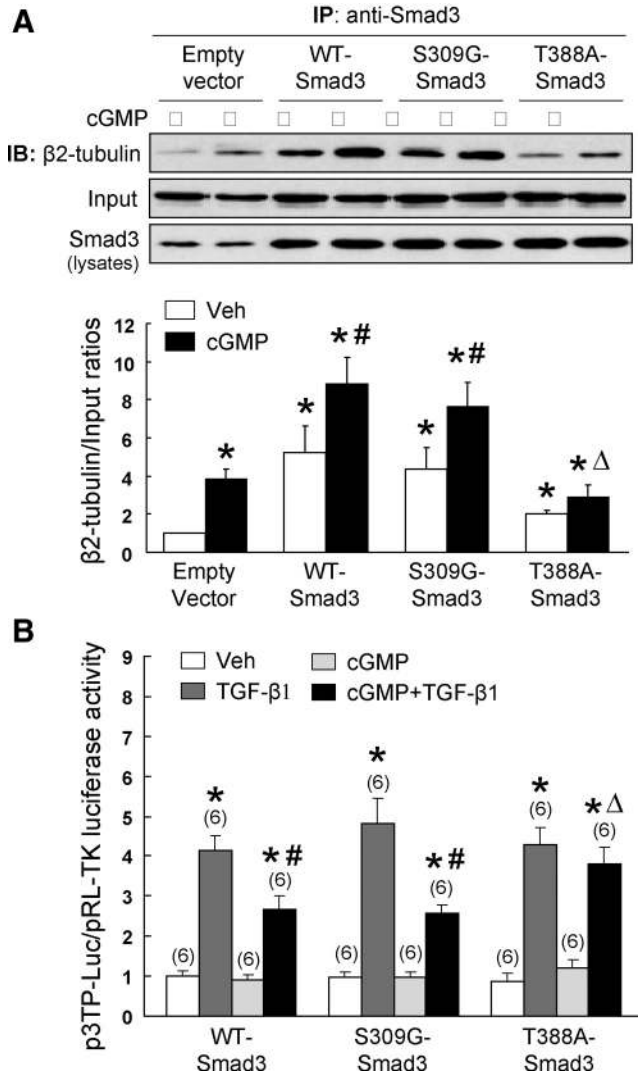

FIG. 4. Mutation of Smad3 at the Thr388 residue attenuates cGMP-induced Smad3 binding to β2-tubulin and abolishes the inhibitory effect of cGMP on TGF-β-induced PAI-1 transcription. A, Serum-starved HEK293 cells were transiently transfected with wild-type Smad3 (WT-Smad3), S309G-Smad3, T388A-Smad3, or empty vector. After 72 h, serum-starved cells were treated with cGMP (0.5 mM) for 1 h. Whole cell extracts were precipitated with anti-Smad3 antibody and then were subjected to IB analysis using anti-β2-tubulin. After IB analysis, the blot was stripped and then probed with anti-Smad3 (input). Same amount of cellular lysate was loaded for IB analysis to detect Smad3 overexpression. Representative IB of the immunoprecititates from three independent experiments are shown. B, PASMC were cotransfected with wild-type and mutant Smad3 plasmids, p3TP-Luc, and pRL-TK. At 48 h after transfection, serum-starved cells were pretreated cGMP for 1 h and followed by TGF-β1 (2 ng/ml) for 24 h. Luciferase activity was measured. Results are means ± SEM; n, Sample size. *, $P < 0.05$ *vs.* vehicle (Veh); #, $P < 0.01$ *vs.* TGF-β1; △, $P < 0.01$ *vs.* cGMP + TGF-β1 in WT-Smad3 group.

Additionally, to test the functional significance of β2-tubulin-mediated Smad3 sequestration in the cytosol in modulating TGF-β-induced stimulation of target gene expression, quiescent PASMC were pretreated with nocodazole or vehicle for 1 h, followed by cGMP treatment for 1 h and then exposed to TGF-β1 for 12 h. PAI-1 mRNA expression was the indicator of activated TGF-β-Smad3 signaling (8). In the absence of nocodazole (control), cGMP pretreatment significantly decreased basal PAI-1 mRNA expression and attenuated the stimulatory effect of TGF-β1 (Fig. 5B), without affecting the viability of the cells (data not shown). However, nocodazole treatment significantly increased PAI-1 mRNA expression in all treatment groups. Further, nocodazole pretreatment significantly enhanced the stimulatory effect of TGF-β1 and abolished the inhibitory effect of cGMP on TGF-β1-induced PAI-1 expression. Similar results were also observed in cells treated with the microtubulin depolymerizer colchicine (Supplemental Fig. 3). Thus, disruption of microtubules abolishes the inhibitory effect of cGMP on TGF-β1-Smad3 signaling in PASMC.

Stabilizing microtubules with pacilitaxel enhances the inhibitory effect of cGMP on TGF-β signaling

We next tested whether stabilizing microtubules with paclitaxel enhances the inhibitory effect of cGMP on TGF-β signaling. Quiescent PASMC were pretreated with paclitaxel or vehicle for 1 h, followed by cGMP treatment for 1 h and then exposed to TGF-β1 for 1 h to detect Smad3 distribution by immunostaining or for 12 h to determine PAI-1 mRNA expression. Immunostaining analysis showed that paclitaxel pretreatment significantly inhibited TGF-β1-induced Smad3 nuclear translocation compared with TGF-β1 alone. Paclitaxel pretreatment potentiated colocalization of Smad3 and β2-tubulin and enhanced the inhibitory effect of cGMP on TGF-β1-induced Smad3 nuclear translocation (Fig. 6A). Quantitative real-time RT-PCR analysis showed that stabilization of microtubulin with either paclitaxel or epothilone B caused a decrease in PAI-1 mRNA expression compared with vehicle-treated control cells. Further, both microtubulin stabilizers inhibited TGF-β1-induced PAI-1 mRNA expression (Fig. 6B and Supplemental Fig. 3). This inhibitory effect was also present in cGMP-pretreated cells, indicating that stabilizing β2-tubulin enhances Smad3 sequestration in the cytosol and thus interferes with TGF-β1 stimulation of target gene expression.

Discussion

We have previously demonstrated that ANP and TGF-β play important counterregulatory roles in the pulmonary vascular adaptation to chronic hypoxia (1–3). In the present study, we characterized a key molecular mechanism for the counterregulation of ANP-cGMP-PKG and TGF-β-Smad3 signaling in isolated PASMC. Using 2D-DIGE and MS analyses, confirmed with Co-IP and immuno-

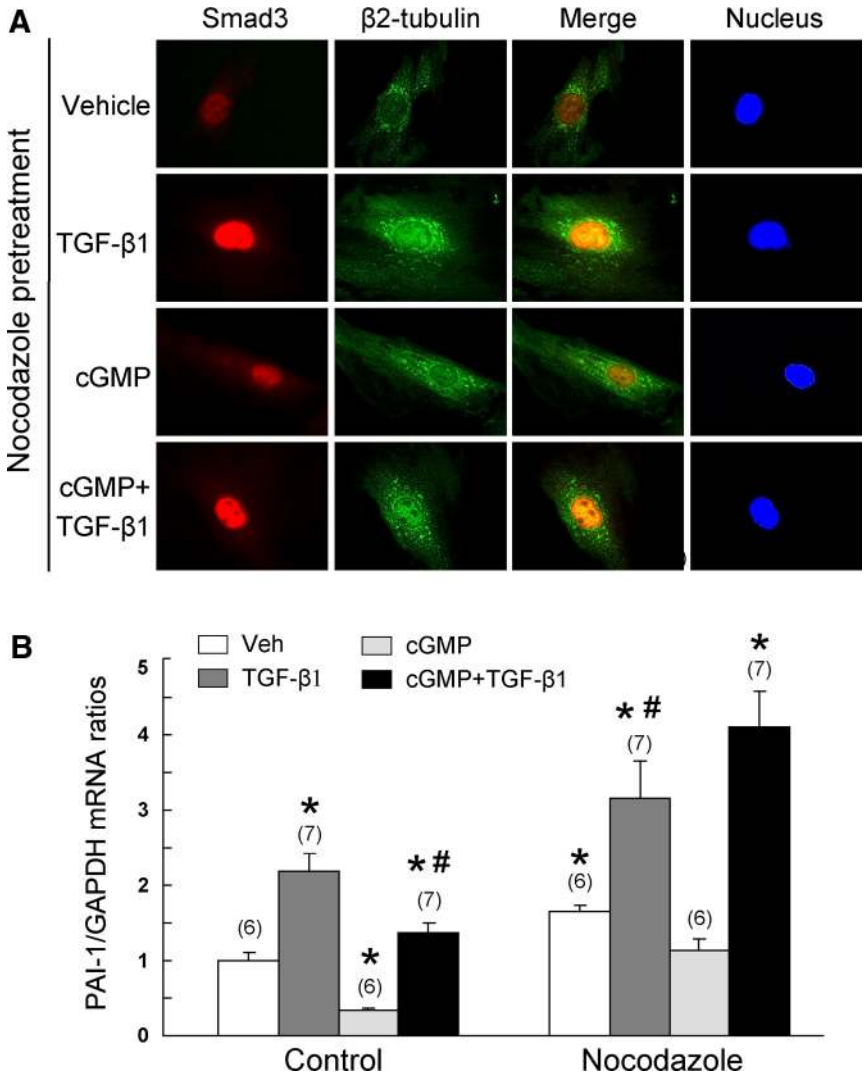

FIG. 5. A, Microtubule disruption abrogates the inhibitory effect of cGMP on TGF-β-induced PAI-1 mRNA expression. Serum-starved PASMC were pretreated with nocodazole (5 μg/ml) or vehicle (control) for 1 h, followed by cGMP (0.5 mM) for 1 h, and then exposed to TGF-β1 (2 ng/ml) for 12 h. B, Total mRNA was extracted. The expression of PAI-1 mRNA was determined by real-time quantitative RT-PCR and normalized using GAPDH mRNA levels as an internal control. Results are means ± SEM; n, Sample size. *, $P < 0.05$ *vs.* vehicle (Veh) group in control; #, $P < 0.01$ *vs.* TGF-β1 group in control; △, $P < 0.01$ *vs.* cGMP + TGF-β1 group in control.

staining, we provide the first evidence that the cytoskeletal protein β2-tubulin plays an important role in mediating the inhibitory effect of ANP-cGMP-PKG activation on TGF-β signaling in isolated PASMC by sequestering Smad3 in the cytosol to prevent its nuclear translocation. We demonstrated that Smad3 binding to cytosolic β2-tubulin in a TGF-β1, cGMP-dependent manner where TGF-β decreases, and cGMP increases Smad3 binding to β2-tubulin. Disruption of β2-tubulin with nocodazole promoted dissociation of Smad3 from β2-tubulin, increased TGF-β-induced Smad3 nuclear translocation and PAI-1 mRNA expression, and abolished the inhibitory effects of cGMP on these processes. In contrast, stabilizing microtubules with paclitaxel increased cytosolic Smad3 binding to β2-tubulin and thus enhanced the inhibitory effect of cGMP on TGF-β-induced Smad3 nuclear translocation and PAI-1 expression.

Smad3 has intrinsic nucleocytoplasmic shuttling capacity and shuttles in and out of the nucleus even in unstimulated cells (9). The subcellular localization of Smad3 is a key feature of the TGF-β-Smad signaling pathway that is determined by the balance between Smad3 nuclear import and export via its constant association/disassociation with various cytoplasmic/nuclear transport factors and retention proteins (10–13). In unstimulated cells, Smad3 resides primarily in the cytosol because of its constitutive export from the nucleus by exportin 4 and binding to cytosolic anchoring proteins (14). Upon ligand stimulation, TGF-β induces phosphorylation of Smad2/3, thus enhancing the interaction of Smad3 with the transporter importin-β1 that recognizes the lysine-rich nuclear localization signal in its mothers against decapentaplegic homology 1 domain, and mediates nuclear import of Smad3 (9). Thus, the fine regulation of Smad3 interaction with cytosolic and nuclear proteins serves as a key mechanism to direct the subcellular distribution of Smad3 and provides dynamic temporal/spatial control of Smad3 signaling in cells.

The cytoskeleton is a platform that modulates intracellular signaling pathways, including TGF-β/Smad signaling, in addition to maintaining cell architecture and regulating the mechanical properties of cells (15–17). Previous studies have shown that Smad2, Smad3, and Smad4 interact with the microtubule network in unstimulated endothelial and epithelial cells (5). Further, the microtubule network has been implicated in trafficking Smad2 to the TGF-β receptor complex for its phosphorylation in both early vertebrate embryos and mammalian cell lines (18). The current study extends these findings to the PASMC and makes the novel observation that cGMP inhibits TGF-β1-induced signal transduction and target gene expression by sequestering Smad3 with β2-tubulin in cytosol.

The finding of cGMP-induced cytosolic sequestration of Smad3 by β2-tubulin provides a partial mechanistic

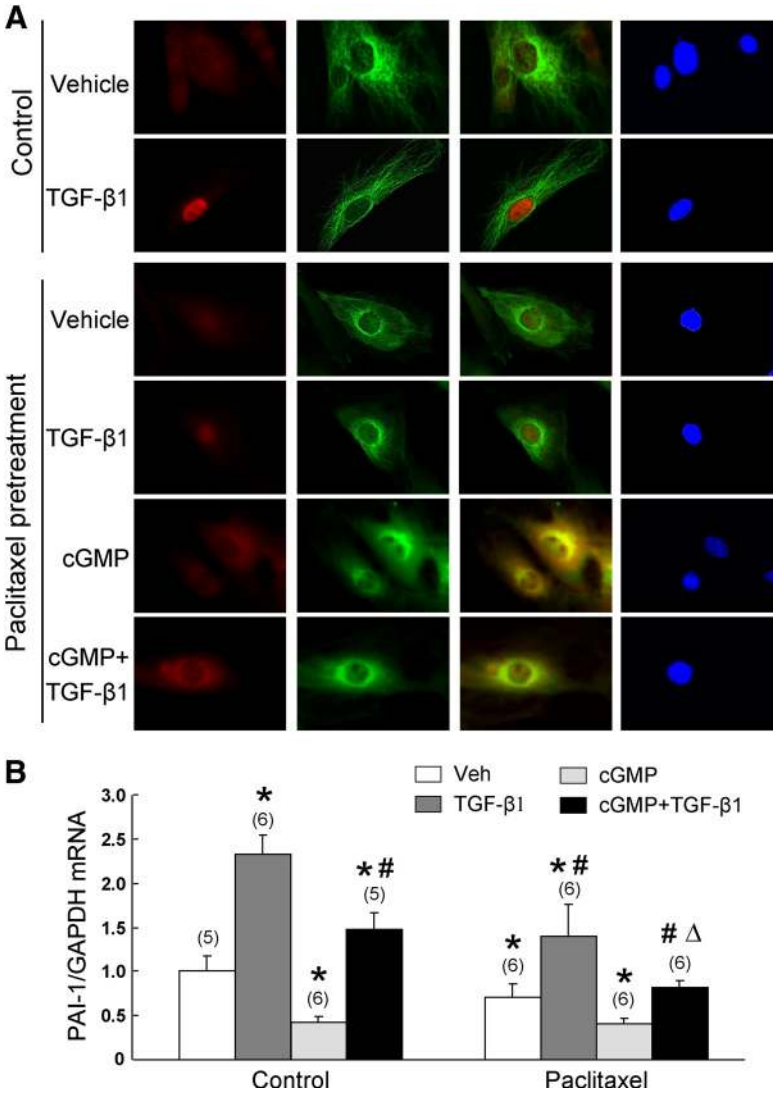

FIG. 6. Microtubule stabilization enhances the inhibition of TGF-β-Smad3 signaling by cGMP. A, Serum-starved PASMC were pretreated with paclitaxel (1 μM), a microtubule stabilizer, or vehicle (control) for 1 h, followed by cGMP (0.5 mM) or vehicle for 1 h, and then exposed to TGF-β1 (2 ng/ml) or vehicle for 1 h. Double immunostaining was performed with anti-Smad3 (*red*) and anti-β2-tubulin (*green*) antibodies. Nucleuses were stained with DAPI. After merging, colocalization is presented in *yellow*. B, Serum-starved PASMC were pretreated with paclitaxel (1 μM) or vehicle (control) for 1 h, followed by cGMP (0.5 μM) for 1 h, and then exposed to TGF-β1 (2 ng/ml) for 12 h. Total mRNA was extracted. The expression of PAI-1 mRNA was determined by real-time RT-PCR and normalized using GAPDH mRNA levels as an internal control. Results are means ± SEM; n, Sample size. *, $P < 0.05$ *vs.* vehicle (Veh) group in control; #, $P < 0.05$ *vs.* TGF-β1 group in control; △, $P < 0.05$ *vs.* cGMP + TGF-β1 group in control.

explanation for our previous observation that ANP-cGMP-PKG activation inhibits nuclear translocation of Smad3 in TGF-β1-treated PASMC and cardiac fibroblasts (3, 7). Our initial efforts to elucidate the mechanisms of this phenomenon tested the focused hypothesis that cGMP-PKG could inhibit TGF-β-induced phosphorylation of Ser423/425 at the C terminus of Smad3 in PASMC (3). In addition, we tested whether cGMP could inhibit Smad3-Smad4 interaction in TGF-β1-treated cells, thus interfering with nuclear translocation of the complex. We found that neither of these hypotheses was correct, *i.e.* cGMP had no effect on phosphorylation of Ser423/425 of Smad3 or on Smad3-Smad4 association in TGF-β1-treated PASMC (Supplemental Fig. 4). Instead, we made the seminal observation that activation of ANP-cGMP-PKG caused hyperphosphorylation of the Ser309 and Thr388 residues in the Mothers against decapentaplegic homology 2 domain of Smad3 (7). These residues are distinct from the C-terminal Ser423/425 residues that are phosphorylated by TGF-β receptor kinase and are induced for the nuclear translocation and downstream signaling of Smad3. The precise mechanism by which cGMP-PKG-induced hyperphosphorylation of Smad3 prevents nuclear translocation of Smad3 and disrupt TGF-β signaling remains unknown, but data from the current study suggest that hyperphosphorylation of Smad3 at the Thr388 residue by cGMP may play a role by facilitating Smad3 binding to cytosolic β2-tubulin.

The current study provides confirmatory evidence that β2-tubulin functions as a cytosolic anchoring protein for Smad3 in the presence of ANP or cGMP. These findings are consistent with previous observations that Smad2/3 can bind to microtubules in unstimulated HL1 cardiomyocytes, whereas overexpression of connexin 43 competes with Smad3 for microtubule binding and thus promotes the release of Smad3 from microtubules, resulting in nuclear accumulation of Smad (6).

The current study demonstrated that disruption of the structure of β2-tubulin abolished the inhibitory effect of cGMP on TGF-β1-induced Smad3 nuclear translocation and PAI-1 expression, supporting the role of β2-tubulin in cGMP-induced inhibition on TGF-β signaling. We also demonstrated that stabilizing microtubule network with paclitaxel not only increased Smad3 colocalization with β2-tubulin in the presence of cGMP but also enhanced the inhibitory effect of cGMP on TGF-β1-induced Smad3 nuclear accumulation and PAI-1 expression. These results supported the concept that increasing the binding of Smad3 to β2-tubulin may be an effective strategy to prevent the excessive profibrotic effects of TGF-β-Smad3 signaling. In support of this concept, recent studies have demonstrated that low-dose paclitaxel treatment effectively ameliorated TGF-β-mediated renal fibrosis in rat

model of unilateral ureteral obstruction and hepatic fibrosis in rat hepatic stellate cells (19, 20). Further, microtubule stabilization has been shown to decrease scar formation and stimulate axonal regeneration after experimental spinal cord injury in rodents via inhibition of TGF-β signaling (21).

In summary, the present study provides the compelling evidence that cytosolic sequestration of Smad3 by binding to β2-tubulin limits its nuclear translocation and mediates the inhibitory effect of cGMP on TGF-β signaling in isolated PASMC. These findings define a novel molecular link that accounts for the functional counterregulatory effect of the ANP-cGMP-PKG pathway on TGF-β-Smad3 signaling.

Materials and Methods

PASMC isolation and culture

PASMC were isolated from distal segments of 10- to 12-wk-old male Sprague Dawley rat pulmonary arteries (second to third branches, 0.1–0.2 mm external diameter) using the explant method as described previously (3). PASMC were used for experiments at passage 3 or 4. Before each study, PASMC were subjected to serum starvation for 24 h. All protocols were approved by the Institutional Animal Care and Use Committee at the University of Alabama at Birmingham and were consistent with the Guide for Care and Use of Laboratory Animals published by the United States National Institutes of Health (Department of Health, Education, and Welfare publication no. 96-01, revised in 2002).

Isolation of cytosolic Smad3 complexes from PASMC

To obtain cytosolic proteins for the differential protomic study, 60 dishes (15-cm dish) of PASMC were treated with vehicle, TGF-β1 (2 ng/ml, 1 h, catalog no. T1654; Sigma-Aldrich, St. Louis, MO) alone, or cGMP (0.5 mM, catalog no. B1381; Sigma-Aldrich) pretreatment for 1 h followed by TGF-β1 (2 ng/ml for 1 h), respectively. Cells were harvested and fractionated using NE-PER nuclear and cytoplasmic extraction reagent (Pierce, Rockford, IL) according to the manufacturer's instructions. The quality of the separation was assessed by Western blot analysis using GAPDH and HDAC1 as markers of the cytosolic and nuclear fractions, respectively. To enrich the cytosolic Smad3 complex, a Crosslink IP kit was used (catalog no. 26147; Pierce) according to the manufacturer's instructions. Briefly, a selective antibody against Smad3 (sc-8332; Santa Cruz Biotechnology, Inc., Santa Cruz, CA) was precoupled to proteinA/G-plus resin and covalently immobilized to the support by cross-linking with disuccinmidyl suberate. The purified cytosolic protein was precleaned with normal rat IgG and Pierce control proteinA/G-plus agarose resin and incubated with the cross-linked anti-Smad3 resin in a 10-ml Pierce centrifuge columns (part no. 89898; Pierce) at 4 C overnight. After washing to remove nonbound proteins from the sample, the Smad3-bound proteins were recovered by dissociation from anti-Smad3 with the supplied elution buffer. Coelution of anti-Smad3 antibody with the Smad3-bound cytosolic proteins was minimized and thus reduced the influence of IgG from anti-Smad3 on the proteomic study. Protease inhibitors (0.5 mM phenylmethylsulfonyl fluoride, 5 mg/ml leupeptin, and 20 μg/ml aprotinin) and phosphotase inhibitors cocktail (Sigma-Aldrich) were added to all buffers except the elution buffer.

2D-DIGE and protein identification by MS

2D-DIGE was performed at Applied Biomics (Hayward, CA), as previously described (22). Briefly, samples were thawed and 2D lysis buffer [7 M urea, 2 M thiourea, 4% 3-[(3-cholamidopropyl)dimethylammonio]-1-propanesulfonate, and 30 mM Tris-HCl (pH 8.8)] was added (10% final concentration). Samples were concentrated using Amicon 3K MWCO spin columns (Millipore, Bedford, MA), and buffer exchange was performed into 2D lysis buffer. Protein concentration was measured using the Bradford assay (Bio-Rad, Hercules, CA). Samples from vehicle, TGF-β1, and cGMP + TGF-β1-treated cells were labeled with Cy2, Cy3, and Cy5, respectively. Labeled samples were mixed and subjected to isoelectric focusing on a 13-cm precast linear immobilized pH gradient strip (pH 3–10; Amersham, Piscataway, NJ). Samples were then separated by 12% SDS-PAGE in the second dimension. Gel images were scanned immediately using Typhoon TRIO (Amersham BioSciences, Piscataway, NJ). The scanned images were analyzed by Image Quant software (version 6.0; Amersham BioSciences), followed by in-gel analysis using DeCyder software (version 6.0; Amersham BioSciences). The fold change of protein expression levels was obtained from in-gel DeCyder analysis.

Based on 2D-DIGE assessment, six protein spots of interest that were expressed differentially in response to cGMP treatment and had the maximal change (increased >2.0-fold in the comparison between cGMP + TGF-β1 and TGF-β1) were picked up using an Ettan spot picker (Amersham BioSciences), digested with trypsin, extracted with 2% trifluoroacetic acid and 40 μl of acetonitrile, and desalted with a ZipTip C18 column (Millipore). Peptides were eluted from the ZipTip and spotted on the matrix-associated laser desorption/ionization plate (model ABI 01-192-6-AB). Matrix-associated laser desorption/ionization-time-of-flight (TOF) MS and TOF/TOF tandem MS/MS were performed on an ABI 4700 mass spectrometer (AB Sciex, Framingham, MA). Candidates with either protein score confidence interval (C.I.)% or Ion C.I.% greater than 95 were considered significant.

Co-IP analysis

To test the effect of TGF-β1 and ANP/cGMP on the interaction between Smad3 and β2-tubulin, quiescent PASMC were treated with ANP (1 μM, catalog no.A8208; Sigma-Aldrich), cGMP (0.5 mM), or vehicle for 1 h, followed by TGF-β1 (2 ng/ml) or vehicle for 1 h. The cells were lysed in Co-IP buffer [120 mM NaCl, 20 mM Tris (pH 7.5), 2 mM EDTA, 1% Triton-X100, 1 mM sodium vanadate, and 10% glycerol] containing 0.5 mM phenylmethylsulfonylfluoride and 20 μg/ml apotinin, and then centrifuged at 12,000 $\times$ g for 15 min at 4 C. Protein concentration was determined by a Bradford-based method (Bio-Rad). After cell lysis, 600 μg of total protein per sample were precleaned with normal rat/mouse IgG and proteinA/G-plus beads (sc-2003; Santa Cruz Biotechnology, Inc.) and then immunoprecipitated with anti-Smad3 (sc-8332; Santa Cruz Biotechnology, Inc.) or anti-β2-tubulin (T8453; Sigma-Aldrich),

respectively, at 4 C for overnight. The bound proteins on proteinA/G-plus beads were washed using Co-IP buffer, centrifuged, eluted with 2× sample loading buffer, boiled at 95 C for 5 min, and stored at −80 C. Each Co-IP experiment was repeated for at least three times.

Western blot analysis

Proteins samples were separated by 10% SDS-PAGE and transferred to polyvinylidene difluoride membrane, as described previously (3). Blots were probed with anti-Smad3, anti-GAPDH (sc-32233; Santa Cruz Biotechnology, Inc.), anti-HDAC1 (sc-7872; Santa Cruz Biotechnology, Inc.), anti-β-actin (sc-47778; Santa Cruz Biotechnology, Inc.) and anti-β2-tubulin primary antibodies, and a horseradish peroxidase-conjugated secondary antibody, respectively. Bands were visualized by use of a Super Western Sensitivity Chemiluminescence Detection System (Pierce). Autoradiographs were quantitated by densitometry (ImageJ; NIH, Bethesda, MD).

Colocalization analysis by immunofluorescence staining

To detect whether Smad3 colocalize with β2-tubulin in PASMC, cells were seeded on glass coverslips. Indirect immunofluorescence staining was carried out, as described previously (23). Quiescent PASMC were pretreated with microtubule depolymerizer nocodazole (5 μg/ml, catalog no. M1404; Sigma-Aldrich), microtubule stabilizer paclitaxel (1 μM, catalog no. T1972; Sigma-Aldrich), or vehicle for 1 h, followed by cGMP (0.5 mM) for 1 h and then exposed to TGF-β1 (2 ng/ml) for additional 1 h. The treated cells were washed, fixed with 4% formaldehyde, and permeabilized with 0.5% Triton X-100. After washing with PBS, cells were blocked with 10% normal goat serum and then incubated with anti-Smad3, anti-β2-tubulin, or normal rabbit/mouse IgG at 4 C for overnight. The slides were incubated with a Texas-red-conjugated antirabbit secondary antibody (1:100, catalog no. TI-1000; Vector Laboratories, Inc., Burlingame, CA) and a fluorescein-conjugated antimouse secondary antibody (1:100, catalog no. FI-2000; Vector Laboratories, Inc.) for 1 h at room temperature. Nuclei were stained with 4′,6-diamidino-2-phenylindole (DAPI) (50 ng/ml) in PBS for 15 min. Coverslips were washed, mounted with 90% glycerol, and visualized by fluorescence microscopy (×400). To provide a valid comparison, identical acquisition parameters were used for all observations. Images were randomly acquired from different fields.

Site-directed mutagenesis and transfection

The full-length (wild type) human Smad3 were subcloned into pMSCV-neo vector (Xu Cao, University of Alabama at Birmingham). Smad3 mutants at the Ser309 (S309G) and Thr388 (T388A) sites were constructed using the QuikChange Site-Directed Mutagenesis kit (Stratagene, La Jolla, CA), according to the manufacturer's protocol, and their sequences confirmed by DNA sequencing. For overexpression of wild-type Smad3 and mutant Smad3 in HEK293 cells, cells were grown in 100-mm dishes to approximately 70% confluence and were transfected 15 μg of plasmids of Smad3, mutant Smad3, or pMSCV-neo empty vector using Lipofectamine LTX with Plus (Invitrogen, Carlsbad, CA). After 72 h of transfection, serum-starved cells were treated with vehicle or cGMP (0.5 mM) for 1 h and then harvested. Whole cell lysates were used for Co-IP analysis using a selective antibody against Smad3.

Luciferase study

To test the functional effects of the mutation of Smad3 at Ser309 and Thr388 on cGMP-induced inhibition of TGF-β/Smad3 signaling, quiescent PASMC were transiently cotransfected with a TGF-β-responsive p3TP-Lux plasmid that contains the −740/−636 region of the PAI-1 promoter bearing the −730 CAGA box, a pRL-TK plasmid (as a control for transfection efficiency) and wild-type Smad3, S309G-Smad3, T388A-Smad3, or empty vector using the Lipofectamine LTX with Plus Transfection Reagent (Invitrogen). At 48 h after transfection, PASMC were treated with TGF-β1 (2 ng/ml) or vehicle for 24 h. PASMC were harvested, and luminescence from transfected PASMC was quantified by measuring firefly/Renilla luciferase activity using the Dual-Luciferase Reporter Assay System (Promega, Madison, WI).

Real-time quantitative RT-PCR analysis

To determine the effects of cGMP, nocodazole/colchicine (catalog no. C9754; Sigma-Aldrich) and paclitaxel/epothilone B (catalog no.E2656; Sigma-Aldrich) on TGF-β1-induced PAI-1 mRNA expression, quiescent PASMC were pretreated with nocodazole (5 μg/ml)/colchicine (1 μM), paclitaxel (1 μM)/epothilone B (50 ng/ml), or vehicle for 1 h, followed by cGMP (0.5 mM) for 1 h and then exposed to TGF-β1 (2 ng/ml) for additional 12 h. Total RNA was extracted using TRIzol Reagent (catalog no. 15596-018; Invitrogen). The purified RNA was reverse transcribed to cDNA using the SuperScript III First-Strand Synthesis System (catalog no. 18080-051; Invitrogen). cDNA was amplified by real-time quantitative PCR using the SYBR Green RT-PCR kit (part no. 4309155; Applied Biosystems, Foster City, CA) in a Bio-Rad iCycler with specific primers of rat PAI-1 (forward, 5′-GCC CTA CCA CGG CGA AAC C-3′ and reverse, 5′-AGG ATG AGG AGG CGG GGC AG-3′) and rat GAPDH (forward, 5′-ATT CTT CCA CCT TTG ATG C-3′ and 5′-TGG TCC AGG GTT TCT TAC T-3′) (Invitrogen). In addition, the expression of PAI-1 mRNA in HEK293 cells was measured using specific primers of human PAI-1 (forward, 5′-TCC AGC CCT CAC CTG CCT AGT C-3′ and reverse, 5′-ACC TGC TGA AAC ACC CTC ACC CC-3′) and human 18S (forward, 5′-GAG AAA CGG CTA CCA CAT CC-3′ and 5′-CAC CAG ACT TGC CCT CCA-3′) (Invitrogen). Relative RNA levels were calculated using the iCycler software (Bio-Rad) and normalized using GAPDH or 18S RNA.

Statistical analysis

Results were expressed as mean ± SEM. Analyses were carried out using the SigmaStat statistical package (Jandel Scientific softwave). Our primary statistical test was one-way ANOVA. If ANOVA results were significant, a *post hoc* comparison among groups was performed with the Newman-Keuls test. A P value of less than 0.05 was considered statistically significant.

Acknowledgments

Address all correspondence and requests for reprints to: Yiu-Fai Chen, Ph.D., Department of Medicine, University of Alabama at Birmingham, Zeigler Research Building 1008, 703 19th Street South, Birmingham, Alabama 35294. E-mail: yfchen@mab.edu.

This work was supported, in part, by National Heart, Lung, and Blood Institute Grants HL080017, HL044195 (to Y.-F.C.),

and HL07457 (to S.O.) and by American Heart Association Grants 10POST3180007 (to K.G.) and 09BGIA2250367 (to D.X.).

Disclosure Summary: The authors have nothing to disclose.

References

1. **Chen YF, Feng JA, Li P, Xing D, Ambalavanan N, Oparil S** 2006 Atrial natriuretic peptide-dependent modulation of hypoxia-induced pulmonary vascular remodeling. Life Sci 79:1357–1365
2. **Chen YF, Feng JA, Li P, Xing D, Zhang Y, Serra R, Ambalavanan N, Majid-Hassan E, Oparil S** 2006 Dominant negative mutation of the TGF-β receptor blocks hypoxia-induced pulmonary vascular remodeling. J Appl Physiol 100:564–571
3. **Li P, Oparil S, Novak L, Cao X, Shi W, Lucas J, Chen YF** 2007 ANP signaling inhibits TGF-β-induced Smad2 and Smad3 nuclear translocation and extracellular matrix expression in rat pulmonary arterial smooth muscle cells. J Appl Physiol 102:390–398
4. **Mascanfroni I, Montesinos Mdel M, Susperreguy S, Cervi L, Ilarregui JM, Ramseyer VD, Masini-Repiso AM, Targovnik HM, Rabinovich GA, Pellizas CG** 2008 Control of dendritic cell maturation and function by triiodothyronine. FASEB J 22:1032–1042
5. **Dong C, Li Z, Alvarez Jr R, Feng XH, Goldschmidt-Clermont PJ** 2000 Microtubule binding to smads may regulate TGF-β activity. Mol Cell 5:27–34
6. **Dai P, Nakagami T, Tanaka H, Hitomi T, Takamatsu T** 2007 Cx43 mediates TGF-β signaling through competitive smads binding to microtubules. Mol Biol Cell 18:2264–2273
7. **Li P, Wang D, Lucas J, Oparil S, Xing D, Cao X, Novak L, Renfrow MB, Chen YF** 2008 Atrial natriuretic peptide inhibits transforming growth factor-β-induced smad signaling and myofibroblast transformation in mouse cardiac fibroblasts. Circ Res 102:185–192
8. **Li G, Heaton JH, Gelehrter TD** 2006 Role of steroid receptor coactivators in glucocorticoid and transforming growth factor β regulation of plasminogen activator inhibitor gene expression. Mol Endocrinol 20:1025–1034
9. **Hill CS** 2009 Nucleocytoplasmic shuttling of Smad proteins. Cell Res 19:36–46
10. **Chen X, Xu L** 2010 Specific nucleoporin requirement for smad nuclear translocation. Mol Cell Biol 30:4022–4034
11. **Moustakas A, Heldin CH** 2009 The regulation of TGF-β signal transduction. Development 136:3699–3714
12. **Dai F, Lin X, Chang C, Feng XH** 2009 Nuclear export of Smad2 and Smad3 by RanBP3 facilitates termination of TGF-β signaling. Dev Cell 16:345–357
13. **Varelas X, Sakuma R, Samavarchi-Tehrani P, Peerani R, Rao BM, Dembowy J, Yaffe MB, Zandstra PW, Wrana JL** 2008 TAZ controls Smad nucleocytoplasmic shuttling and regulates human embryonic stem-cell self-renewal. Nat Cell Biol 10:837–848
14. **Kurisaki A, Kurisaki K, Kowanetz M, Sugino H, Yoneda Y, Heldin CH, Moustakas A** 2006 The mechanism of nuclear export of Smad3 involves exportin 4 and Ran. Mol Cell Biol 26:1318–1332
15. **Moustakas A, Heldin CH** 2008 Dynamic control of TGF-β signaling and its links to the cytoskeleton. FEBS Lett 582:2051–2065
16. **Samarakoon R, Goppelt-Struebe M, Higgins PJ** 2010 Linking cell structure to gene regulation: signaling events and expression controls on the model genes PAI-1 and CTGF. Cell Signal 22:1413–1419
17. **Etienne-Manneville S** 2010 From signaling pathways to microtubule dynamics: the key players. Curr Opin Cell Biol 22:104–111
18. **Batut J, Howell M, Hill CS** 2007 Kinesin-mediated transport of smad2 is required for signaling in response to TGF-β ligands. Dev Cell 12:261–274
19. **Zhang D, Sun L, Xian W, Liu F, Ling G, Xiao L, Liu Y, Peng Y, Haruna Y, Kanwar YS** 2010 Low-dose paclitaxel ameliorates renal fibrosis in rat UUO model by inhibition of TGF-β/Smad activity. Lab Invest 90:436–447
20. **Zhou J, Zhong DW, Wang QW, Miao XY, Xu XD** 2010 Paclitaxel ameliorates fibrosis in hepatic stellate cells via inhibition of TGF-β/Smad activity. World J Gastroenterol 16:3330–3334
21. **Hellal F, Hurtado A, Ruschel J, Flynn KC, Laskowski CJ, Umlauf M, Kapitein LC, Strikis D, Lemmon V, Bixby J, Hoogenraad CC, Bradke F** 2011 Microtubule stabilization reduces scarring and causes axon regeneration after spinal cord injury. Science 331:928–931
22. **Huang NF, Kurpinski K, Fang Q, Lee RJ, Li S** 2011 Proteomic identification of biomarkers of vascular injury and restenosis. Am J Transl Res 3:139–148
23. **Gong K, Li Z, Xu M, Du J, Lv Z, Zhang Y** 2008 A novel protein kinase A-independent, β-arrestin-1-dependent signaling pathway for p38 mitogen-activated protein kinase activation by β2-adrenergic receptors. J Biol Chem 283:29028–29036